Cellular and Molecular Neurobiology (2018) 38:1557–1563
https://doi.org/10.1007/s10571-018-0620-7

BRIEF COMMUNICATION

# A Novel Microfluidic Device-Based Neurite Outgrowth Inhibition Assay Reveals the Neurite Outgrowth-Promoting Activity of Tropomyosin Tpm3.1 in Hippocampal Neurons

**Holly Stefen[1,2] · Amin Hassanzadeh-Barforoushi[3,4] · Merryn Brettle[1] · Sandra Fok[1] · Alexandra K. Suchowerska[1] · Nicodemus Tedla[5] · Tracie Barber[3] · Majid Ebrahimi Warkiani[6,7] · Thomas Fath[1,2,8]**

Received: 6 August 2018 / Accepted: 6 September 2018 / Published online: 14 September 2018


## Abstract

Overcoming neurite inhibition is integral for restoring neuronal connectivity after CNS injury. Actin dynamics are critical for neurite growth cone formation and extension. The tropomyosin family of proteins is a regarded as master regulator of actin dynamics. This study investigates tropomyosin isoform 3.1 (Tpm3.1) as a potential candidate for overcoming an inhibitory substrate, as it is known to influence neurite branching and outgrowth. We designed a microfluidic device that enables neurons to be grown adjacent to an inhibitory substrate, Nogo-66. Results show that neurons, overexpressing hTpm3.1, have an increased propensity to overcome Nogo-66 inhibition. We propose Tpm3.1 as a potential target for promoting neurite growth in an inhibitory environment in the central nervous system.

**Keywords** Tropomyosins · Neurite outgrowth inhibition · Microfluidic systems · NogoA

## Introduction

Neuronal regeneration in the injured or diseased central nervous system (CNS) is limited due to a large range of intrinsic and extrinsic factors that inhibit the regrowth of neurites from injured neurons. Cytoskeletal reorganisation enables dynamic extension and exploration of neurites, which then form connections with other neurons (Acebes and Ferrus 2000). Extracellular cues, coupled with the reorganisation of the actin cytoskeleton, drive the extension of neurites at the growth cone. Actin-associated protein tropomyosin (Tpm) is a key regulator of neuritogenesis and neurite branching (Curthoys et al. 2014; Fath et al. 2010; Schevzov et al. 2005). In mammals, over 40 Tpm isoforms have been identified, arising from the alternative splicing of four different genes (*Tpm1-4*) [for review, see (Geeves et al. 2015)], with isoforms from three genes (*Tpm1, Tpm3*

Holly Stefen, Amin Hassanzadeh-Barforoushi and Merryn Brettle are co-first authors.

Majid Ebrahimi Warkiani and Thomas Fath are senior authors.

**Electronic supplementary material** The online version of this article (https://doi.org/10.1007/s10571-018-0620-7) contains supplementary material, which is available to authorized users.

✉ Majid Ebrahimi Warkiani
majid.warkiani@uts.edu.au

✉ Thomas Fath
thomas.fath@mq.edu.au

[1] Neurodegenerative and Repair Unit, School of Medical Science, UNSW Sydney, Sydney, NSW, Australia

[2] Neuron Culture Core Facility (NCCF), University of New South Wales, Sydney, NSW, Australia

[3] School of Mechanical and Manufacturing Engineering, University of New South Wales, Sydney, NSW 2052, Australia

[4] Cancer Division, Garvan Institute of Medical Research/The Kinghorn Cancer Centre, Sydney, NSW 2010, Australia

[5] Inflammation Research, School of Medical Sciences, University of New South Wales, Sydney, NSW, Australia

[6] School of Biomedical Engineering, University of Technology Sydney, Sydney, NSW 2007, Australia

[7] Institute of Molecular Medicine, Sechenov First Moscow State University, Moscow 119991, Russia

[8] Faculty of Medicine and Health Sciences, Dementia Research Centre, Macquarie University, Sydney, NSW 2019, Australia

and *Tpm4*) found to be expressed in neurons [for review, see (Schevzov et al. 2012) and (Brettle et al. 2016)]. Tpms form a coiled-coil dimer along the major α-helical groove of actin filaments, thereby regulating the access of other actin-binding proteins to the filament in an isoform-dependent manner [for review, see (Gunning et al. 2015)]. Tpm isoform Tpm3.1 has long been associated with promoting neurite outgrowth and axonal extension (Schevzov et al. 2005, 2008; Weinberger et al. 1996; Fath et al. 2010). In particular, the overexpression of human Tpm3.1 (hTpm3.1) results in enlarged growth cones (Schevzov et al. 2005), with increased actin polymer (Schevzov et al. 2008), an increase in the number of dendrites and increased axonal branching. The regulation of neurite outgrowth by tropomyosins in an inhibitory substrate context has not yet been studied. In the current study, we investigate hTpm3.1 overexpression on neurite outgrowth in the presence of Nogo66. Myelin-associated inhibitor NogoA is a potent inhibitor of neurite outgrowth of central nervous system neurons (Chen et al. 2000). The small peptide sequence Nogo-66 of NogoA leads to neurite growth inhibition via signalling through the RhoA/ROCK pathway, modulating actin filament dynamics (Fournier et al. 2003; Mi et al. 2004). The binding affinity of Nogo-66 to its receptors NgR1 and PirB has Kd values of $1.2 \pm 0.4$ and $2.4 \pm 0.6$, respectively (Huebner et al. 2011). Nogo-66 possesses nanomolar potency for inhibiting growth cone collapse and neurite growth with a reported median effective concentration ($EC_{50}$) of 50 nM (GrandPre et al. 2000). We have previously validated the use of recombinant Nogo-66 for its use in studying neurite outgrowth inhibition in vitro, using mouse and human cortical neurons (An et al. 2016).

Microfluidic devices have increasingly been recognised for their potential in deciphering the function of nerve cells in the healthy, injured and ageing brain [for review, see (Osaki et al. 2017)]. Microfluidic devices have solved issues of difficulty in operation, costs of experiments and low throughput, by providing rapid and precise spatiotemporal control over the neurons' microenvironment. Perhaps, one of the most promising applications of microfluidics in neuron research is investigating the mechanism of neuronal injury due to physical (Hosmane et al. 2011; Hellman et al. 2010) or chemical stimuli (Li et al. 2012; Yang et al. 2009). However, many microfluidic devices compartmentalise axon outgrowth to predefined channel shapes. In addition, since axon outgrowth occurs inside the microchannels, studying the effect of substrate-bound cues is not possible. Here, we describe a new microfluidic device based on our previously developed system for studying cell–cell interactions (Hassanzadeh-Barforoushi et al. 2016). This novel device is fabricated, using conventional soft-lithography method and can be simply operated with a standard hand-held pipette with no previous expertise. Using this device, we show for the first time that overexpression of hTpm3.1 overcomes the neurite outgrowth inhibition activity of the CNS-derived inhibitor NogoA.

## Materials and Methods

See supporting information.

## Results and Discussion

First we optimised the previously developed microfluidic device (Hassanzadeh-Barforoushi et al. 2016), characterised by intercalating channels, for the use of neurons, cultured at low density (Fath et al. 2009). We thereby established a microfluidic device-based assay, which allows rapid and precise patterning of neurons and an inhibitory substrate in an intercalating pattern (Fig. 1a–c). Neurite outgrowth was determined by measuring a straight line from the outer boundary of the plated cell layer to the tip of the growth cone (Fig. 1d). The distance from the edge of the plated cell layer to the GST-Nogo-66-coated region, also shown in (Fig. 1d), is 175 µm. GST-Nogo-66, injected into the device, adhered to the coverslip in the defined channel pattern, and was persistent over a 7-day period, as confirmed by measuring of fluorescence intensity, after immunostaining with an antibody, directed against GST (Fig. 2a–c). By seeding a cortical support ring around the perimeter of the culture dish (Fath et al. 2009), the hippocampal neurons plated onto the centre of the coverslip in the pattern dictated by the microfluidic device remain viable, as measured at 3 and 7 DIV (Fig. 2d–l). At 3 DIV, $93.8 \pm 1.1\%$ were alive with support ring versus $43.3 \pm 5.8\%$ without support ring and at 7 DIV, $90.5 \pm 1.7\%$ were alive with support ring versus $34 \pm 10.1\%$ without support ring.

To determine the optimal time point for analysis of neurite growth behaviour, as neurites encounter the GST-Nogo-66-coated area, neurons were fixed at time points from 2 to 7 days in vitro (DIV) (Fig. 2m–s) and measured as mentioned above (Fig. 1d). Neurite outgrowth was found to reach the GST-Nogo-66 region between 4 DIV and 5 DIV (Fig. 2s). Therefore, live-imaging analysis of neurite outgrowth behaviour was analysed over a 24-h time period from 4 DIV to 5 DIV.

Neurite growth rates of wild-type and hTpm3.1-overexpressing neurons were measured in the growth-permissive area (labelled $-2$ and $-3$, Fig. 3a) and the GST-Nogo-66 region (labelled $-1$ and 1, Fig. 3a). Our data show that the overexpression of hTpm3.1 significantly slows the rate of neurite outgrowth from $0.85 \pm 0.07$ to $0.57 \pm 0.05$ µm/min (Fig. 3b). However, while neurite growth rate of wild-type neurons slows upon reaching the GST-Nogo-66-coated region (i.e., $0.85 \pm 0.07$ µm/min outside GST-Nogo-66

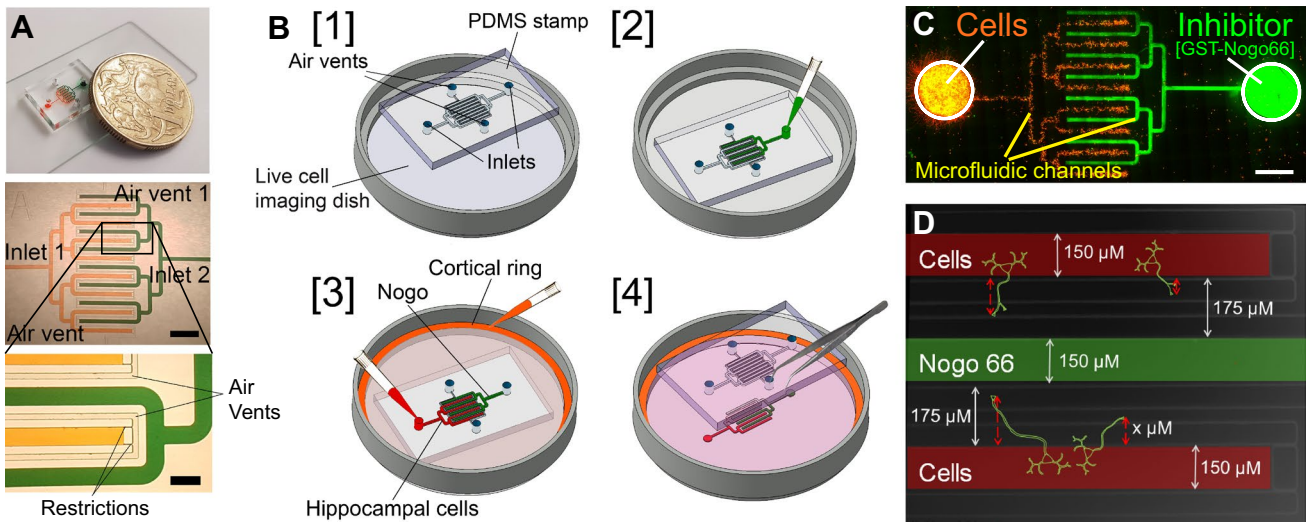


**Fig. 1** Design of microfluidic device. **A** Photo of microfluidic device for scale (top). Detailed schematic of microfluidic configuration with intercalating channels shown in yellow and green (middle) and enlarged image of area outlined showing device properties (bottom). Scale bars = 1 mm (middle) and 200 µm (bottom). **b** Schematic showing device being placed into live cell imaging dish B[1], loading of GST-Nogo-66 substrate (green) into channels on the right (B[2]), seeding of hippocampal cells into channels on the left (red) and cortical cells into a support ring (orange)(B[3]) and removal of the microfluidic device once cells are attached (B[4]). **c** Immunofluorescence image, displaying experimental loading of devices with GST-Nogo-66 inhibitory substrate coating on the right (green) and primary hippocampal cells on the left (orange). Scale bar = 1.5 mm. **d** Brightfield image of microfluidic device (white outline) with a schematic overlay showing channel dimensions and distances between intercalating channels. The schematic demonstrates how the lengths of neurites were measured

coated region and 0.51 ± 0.05 µm/min within GST-Nogo-66 coated region), neurites of hTpm3.1-overexpressing neurons appear largely insensitive to the inhibitory substrate, showing no significant change in their growth rate upon entering the GST-Nogo-66-coated region. A key property of Tpm3.1 is its ability to influence actin filament dynamics by regulating the interaction of other actin-associating proteins with the filament. For example, Tpm3.1 regulates actin dynamics, at least in part, by inhibition of ADF/cofilin as shown in Bryce et al. (2003) and Robaszkiewicz et al. (2016). This inhibition is likely through the regulation of signalling cues, upstream of ADF/cofilin, since reconstituting the actin polymerization machinery containing actin, cofilin and tropomyosin in vitro does not show a direct inhibition of cofilin activity (Bonello et al. 2016; Janco et al. 2016). ADF/cofilin is suggested to be an integral contributor to actin turnover, regulating neurite extension (Endo et al. 2003; Meberg and Bamburg 2000). By preventing ADF/cofilin from severing actin filaments, increased stabilisation of the actin filament population could lead to reduced growth cone advance and a reduced rate of neurite outgrowth, which we see in our assay system (Fig. 3b).

We then determined the proportion of wild-type and hTpm3.1-overexpressing neurons that extend their neurites into the GST-Nogo-66-coated region. We found a significant difference in the ability of wt and hTpm3.1 overexpressing neurons to overcome the GST-Nogo-66 substrate (Fig. 3c). Compared to wt neurons, neurons overexpressing hTpm3.1 show a much greater propensity to extend into and past the GST-Nogo-66-coated region (Fig. 3c). This is indicated by a 1.7- and 3.9-fold increase in the number of neurites tips located in (regions − 1 and 1) and past (regions 2 and 3) the GST-Nogo-66-coated area, respectively. No differences in neurite outgrowth were observed between the two groups in the absence of GST-Nogo-66 (Fig. 3c).

We have previously shown that Tpm3.1 regulates neurite outgrowth in neurons in an isoform-specific manner, which are not exposed to extracellular guidance cues (Schevzov et al. 2008, 2012; Fath et al. 2010; Curthoys et al. 2014). Our findings here suggest that Tpm3.1 may have an important function in controlling how neurons respond to external cues for neurite outgrowth. NogoA has been shown to mediate neurite inhibition by signalling through the RhoA/ROCK pathway, leading to the activation of the actin filament severing protein ADF/cofilin and subsequent depolymerization of actin filaments in the growth cones and eventually growth cone collapse (Niederost et al. 2002; Hsieh et al. 2006; Fournier et al. 2003). One may speculate that Tpm3.1 counteracts the neurite growth-inhibiting effect of Nogo-66 by inhibiting ADF/cofilin activity, decoupling the extracellular growth-inhibitory signal of NogoA from the depolymerization of the actin cytoskeleton in the growth cones.

Nogo-66 has been shown to be an effective inhibitor for neurite outgrowth in a wide range of different neuronal

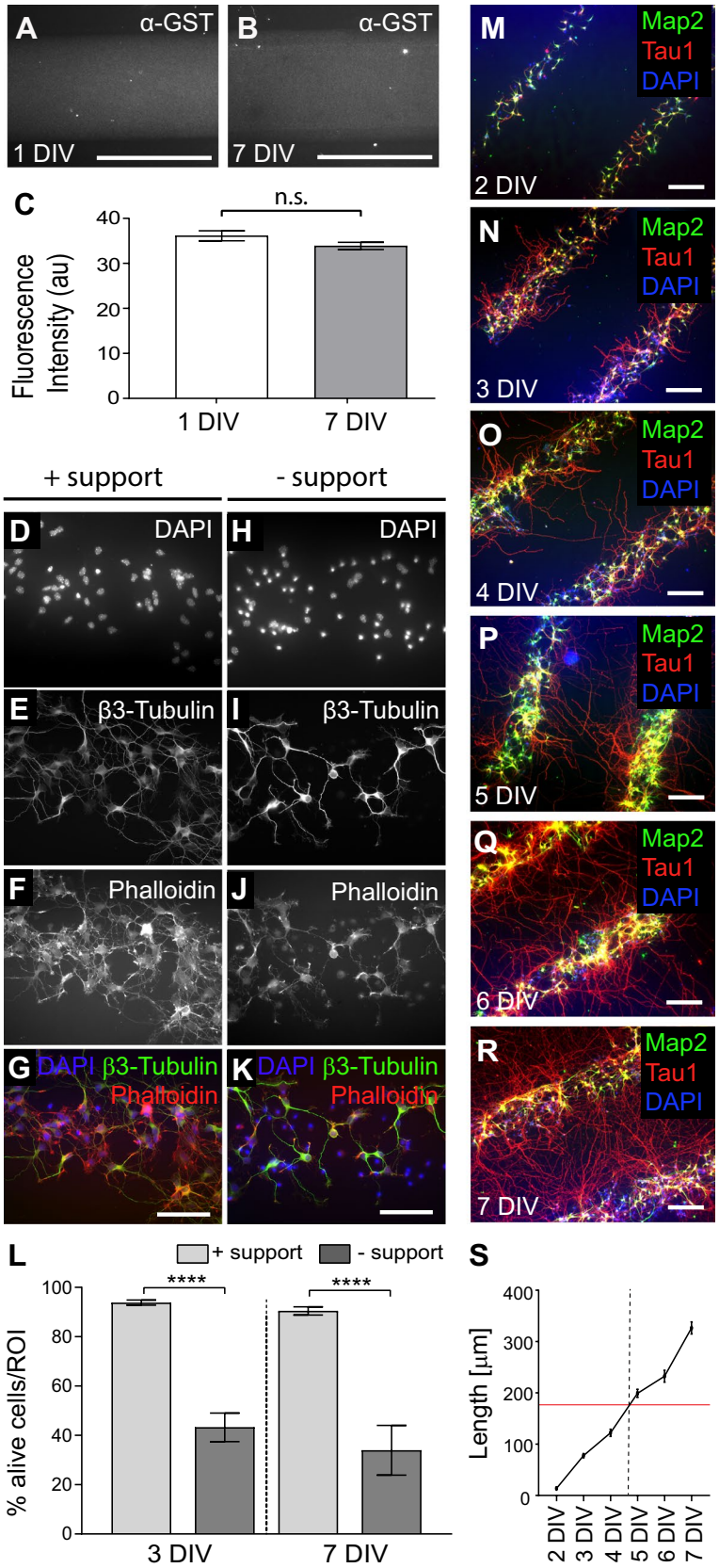


**Fig. 2** Validation of GST-Nogo-66 coating (**a**–**c**), cell viability (**d**–**l**) and optimization of neurite outgrowth assay (**m**–**s**). **a, b** Fluorescence images of GST-Nogo-66 coating in channel pattern defined by microfluidic device at 1 day in vitro (DIV) and 7 DIV, scale bars = 150 µm. **c** Quantification of fluorescence intensity of GST-Nogo-66. Graph shows mean ± SEM. Unpaired *t* test. *n* = 20. **d**–**k** Fluorescence images of hippocampal neurons at 3 DIV, plated with (**d, e, f, g**) or without (**h, i, j, k**) a cortical support ring. Scale bars = 100 µm. **l** Quantification of cortical support ring experiments at 3 and 7 DIV. Graph depicts the mean percentage of alive cells per region of interest ± SEM. Unpaired *t* tests. *n* = 10–11. *P* value ****$P < 0.0001$. **m**–**r** Immunofluorescence images of neurite outgrowth from 2 DIV to 7 DIV. **s** Quantification of neurite lengths from time points in (**m**–**r**). Graph shows mean ± SEM. The distance between intercalating channels (175 µm) is indicated by the red line. The time point at which neurites reach the GST-Nogo-66-coated substrate is depicted by the black, dashed line. *n* = 23 (2 DIV), 120 (3 DIV), 119 (4 DIV), 125 (5 DIV), 95 (6 DIV), 43 (7 DIV). Scale bars = 200 µm

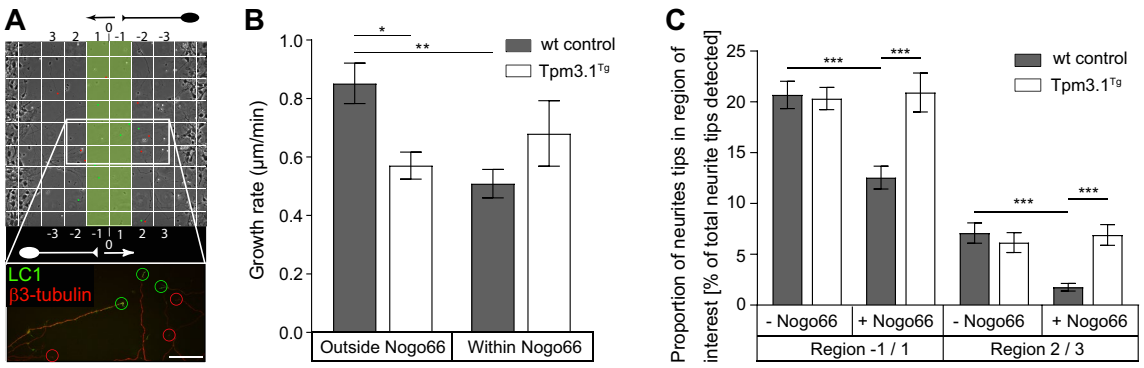


**Fig. 3** Neurite outgrowth promoting activity of Tpm3.1 in the presence of GST-Nogo-66. **a** Phase contrast image of hippocampal neurons at the completion of live recording. Grid overlay shows the division of cell culture area into regions of interest based on distance from GST-Nogo-66 substrate (pseudo-coloured green). Insert shows magnified region containing hTpm3.1 overexpressing and wt neurites circled in green and red, respectively. Scale bar = 50 µm. **b** Quantification of neurite growth rate within GST-Nogo-66-coated areas and non-coated areas. Tukey's multiple comparisons test. Shown are mean ± SEM. $n \geq 12$. $P$ value $^{*}P = 0.016$, $^{**}P < 0.01$. **c** Quantification of the proportion of neurite tips within region −1/1 and region 2/3 in the presence (+Nogo66) or absence (−Nogo66) of GST-Nogo-66. The graph depicts mean of proportions of total number of cells ± SEM. Bonferroni's multiple comparison test. $n = 20$. $P$ value $^{*}P = 0.0475$, $^{***}P = 0.0003$, $^{****}P < 0.0001$

populations, including chicken dorsal root ganglion neurons, chicken retinal neurons, mouse cerebellar granule neurons, human cortical neurons and mouse cortical neurons (An et al. 2016; Fournier et al. 2001). Our data, using Nogo-66 as an inhibitor in in vitro assays, show neurite inhibition in both cortical (An et al. 2016) and hippocampal neurons (data from the current study). Detailed studies on the expression profile of the Nogo receptor NgR1 and its co-receptors Lingo-1 and $p75^{NTR}$ show a wide distribution of expression in the brain (Barrette et al. 2007; Funahashi et al. 2008). A function of increased expression levels of Tpm3.1 in counteracting Nogo66-induced neurite growth inhibition at the level of ADF/cofilin activity would likely lead to a growth-promoting effect in different populations of central nervous system (CNS) neurons. Previous studies from ours and other groups have shown that the regulation of ADF/cofilin activity by Tpm3.1 is isoform specific. While both Tpm3.1 and the Tpm4 gene product Tpm4.2 inhibit ADF/cofilin activity, the Tpm1 gene product Tpm1.12 recruits ADF/cofilin to actin filaments and allows severing of the filaments. Tpm3.1, Tpm4.2 and Tpm1.12 are expressed in developing neurons [for a detailed review, see (Schevzov et al. 2012)]. Therefore, future studies will be required to test the effects of other Tpm isoforms on neurons, extending their process into a growth-inhibitory environment.

The new microfluidic device, used in this study, allows for pharmacological and genetic dissection of the precise mechanisms by which Tpm3.1 overexpression overcomes the inhibitory effect of NogoA on neurite outgrowth in different neuronal populations of CNS neurons. Whether this growth-promoting property of Tpm3.1 is isoform specific, or whether other Tpm isoforms have a similar or opposing effect, remains to be established in future studies. In conclusion, our data provide compelling new evidence that modulating the expression levels of a key regulator of actin filament dynamics in hippocampal neurons is sufficient to overcome the effect of a potent inhibitor of neurite outgrowth in the mammalian CNS. Thereby, our findings may lead to new strategies to promote neurite outgrowth in inhibitory environments and promoting nervous system regeneration.

**Acknowledgements** This work was supported by Project Grant APP1083209 from the Australian National Health and Medical Research Council (NHMRC) (T.F.) and Discovery Project Grant DP180101473 from the Australian Research Council (ARC) (T.F.). We thank Tamara Tomanić (UNSW Sydney) for her constructive feedback and critical reading of the manuscript. This work was performed (in part) at the NSW and South Australian node of the Australian National Fabrication Facility under the National Collaborative Research Infrastructure Strategy to provide nano- and microfabrication facilities for Australia's researchers. M.E.W. would like to acknowledge the support of the Australian Research Council through Discovery Project Grants (DP170103704 and DP180103003) and the National Health and Medical Research Council through the Career Development Fellowship (APP1143377).

**Author Contributions** TF, MEW and TB supervised the project. TF, HS, AH-B and SF designed the research. HS, AH-B, SF and MB performed the research and analysed the data. TF, HS, AH-B and SF wrote the paper. TF, HS, AH-B, AKS, MB and NT edited the paper. All authors read and approved the final manuscript.

## Compliance with Ethical Standards

**Conflict of interest** The authors declare that the research was conducted in the absence of any commercial, financial or non-financial relationships that could be construed as a potential conflict of interest.

**Ethical Approval** All procedures were conducted in accordance with the Australian Code of Practice for the Care and Use of Animals for

Scientific Purposes and were approved by the University of New South Wales Animal Care and Ethics Committee.

## References


Acebes A, Ferrus A (2000) Cellular and molecular features of axon collaterals and dendrites. Trends Neurosci 23(11):557–565

An H, Brettle M, Lee T, Heng B, Lim CK, Guillemin GJ, Lord MS, Klotzsch E, Geczy CL, Bryant K, Fath T, Tedla N (2016) Soluble LILRA3 promotes neurite outgrowth and synapses formation through high affinity interaction with Nogo 66. J Cell Sci. https://doi.org/10.1242/jcs.182006

Barrette B, Vallieres N, Dube M, Lacroix S (2007) Expression profile of receptors for myelin-associated inhibitors of axonal regeneration in the intact and injured mouse central nervous system. Mol Cell Neurosci 34(4):519–538. https://doi.org/10.1016/j.mcn.2006.12.004

Bonello TT, Janco M, Hook J, Byun A, Appaduray M, Dedova I, Hitchcock-DeGregori S, Hardeman EC, Stehn JR, Bocking T, Gunning PW (2016) A small molecule inhibitor of tropomyosin dissociates actin binding from tropomyosin-directed regulation of actin dynamics. Sci Rep 6:19816. https://doi.org/10.1038/srep19816

Brettle M, Patel S, Fath T (2016) Tropomyosins in the healthy and diseased nervous system. Brain Res Bull 126(Pt 3):311–323. https://doi.org/10.1016/j.brainresbull.2016.06.004

Bryce NS, Schevzov G, Ferguson V, Percival JM, Lin JJ, Matsumura F, Bamburg JR, Jeffrey PL, Hardeman EC, Gunning P, Weinberger RP (2003) Specification of actin filament function and molecular composition by tropomyosin isoforms. Mol Biol Cell 14(3):1002–1016

Chen MS, Huber AB, van der Haar ME, Frank M, Schnell L, Spillmann AA, Christ F, Schwab ME (2000) Nogo-A is a myelin-associated neurite outgrowth inhibitor and an antigen for monoclonal antibody IN-1. Nature 403(6768):434–439. https://doi.org/10.1038/35000219

Curthoys NM, Freittag H, Connor A, Desouza M, Brettle M, Poljak A, Hall A, Hardeman E, Schevzov G, Gunning PW, Fath T (2014) Tropomyosins induce neuritogenesis and determine neurite branching patterns in B35 neuroblastoma cells. Mol Cell Neurosci 58C:11–21. https://doi.org/10.1016/j.mcn.2013.10.011

Endo M, Ohashi K, Sasaki Y, Goshima Y, Niwa R, Uemura T, Mizuno K (2003) Control of growth cone motility and morphology by LIM kinase and Slingshot via phosphorylation and dephosphorylation of cofilin. J Neurosci 23(7):2527–2537

Fath T, Ke YD, Gunning P, Gotz J, Ittner LM (2009) Primary support cultures of hippocampal and substantia nigra neurons. Nat Protoc 4(1):78–85

Fath T, Agnes Chan YK, Vrhovski B, Clarke H, Curthoys N, Hook J, Lemckert F, Schevzov G, Tam P, Watson CM, Khoo PL, Gunning P (2010) New aspects of tropomyosin-regulated neuritogenesis revealed by the deletion of Tm5NM1 and 2. Eur J Cell Biol 89(7):489–498

Fournier AE, GrandPre T, Strittmatter SM (2001) Identification of a receptor mediating Nogo-66 inhibition of axonal regeneration. Nature 409(6818):341–346. https://doi.org/10.1038/35053072

Fournier AE, Takizawa BT, Strittmatter SM (2003) Rho kinase inhibition enhances axonal regeneration in the injured CNS. J Neurosci 23(4):1416–1423

Funahashi S, Hasegawa T, Nagano A, Sato K (2008) Differential expression patterns of messenger RNAs encoding Nogo receptors and their ligands in the rat central nervous system. J Comp Neurol 506(1):141–160. https://doi.org/10.1002/cne.21541

Geeves MA, Hitchcock-DeGregori SE, Gunning PW (2015) A systematic nomenclature for mammalian tropomyosin isoforms. J Muscle Res Cell Motil 36(2):147–153. https://doi.org/10.1007/s10974-014-9389-6

GrandPre T, Nakamura F, Vartanian T, Strittmatter SM (2000) Identification of the Nogo inhibitor of axon regeneration as a Reticulon protein. Nature 403(6768):439–444. https://doi.org/10.1038/35000226

Gunning PW, Hardeman EC, Lappalainen P, Mulvihill DP (2015) Tropomyosin—master regulator of actin filament function in the cytoskeleton. J Cell Sci 128(16):2965–2974. https://doi.org/10.1242/jcs.172502

Hassanzadeh-Barforoushi A, Shemesh J, Farbehi N, Asadnia M, Yeoh GH, Harvey RP, Nordon RE, Warkiani ME (2016) A rapid co-culture stamping device for studying intercellular communication. Sci Rep 6:35618. https://doi.org/10.1038/srep35618

Hellman AN, Vahidi B, Kim HJ, Mismar W, Steward O, Jeon NL, Venugopalan V (2010) Examination of axonal injury and regeneration in micropatterned neuronal culture using pulsed laser microbeam dissection. Lab Chip 10(16):2083–2092. https://doi.org/10.1039/b927153h

Hosmane S, Fournier A, Wright R, Rajbhandari L, Siddique R, Yang IH, Ramesh KT, Venkatesan A, Thakor N (2011) Valve-based microfluidic compression platform: single axon injury and regrowth. Lab Chip 11(22):3888–3895. https://doi.org/10.1039/c1lc20549h

Hsieh SH, Ferraro GB, Fournier AE (2006) Myelin-associated inhibitors regulate cofilin phosphorylation and neuronal inhibition through LIM kinase and Slingshot phosphatase. J Neurosci 26(3):1006–1015. https://doi.org/10.1523/JNEUROSCI.2806-05.2006

Huebner EA, Kim BG, Duffy PJ, Brown RH, Strittmatter SM (2011) A multi-domain fragment of Nogo-A protein is a potent inhibitor of cortical axon regeneration via Nogo receptor 1. J Biol Chem 286(20):18026–18036. https://doi.org/10.1074/jbc.M110.208108

Janco M, Bonello TT, Byun A, Coster AC, Lebhar H, Dedova I, Gunning PW, Bocking T (2016) The impact of tropomyosins on actin filament assembly is isoform specific. Bioarchitecture 6(4):61–75. https://doi.org/10.1080/19490992.2016.1201619

Li L, Ren L, Liu W, Wang JC, Wang Y, Tu Q, Xu J, Liu R, Zhang Y, Yuan MS, Li T, Wang J (2012) Spatiotemporally controlled and multifactor involved assay of neuronal compartment regeneration after chemical injury in an integrated microfluidics. Anal Chem 84(15):6444–6453. https://doi.org/10.1021/ac3013708

Meberg PJ, Bamburg JR (2000) Increase in neurite outgrowth mediated by overexpression of actin depolymerizing factor. J Neurosci 20(7):2459–2469

Mi S, Lee X, Shao Z, Thill G, Ji B, Relton J, Levesque M, Allaire N, Perrin S, Sands B, Crowell T, Cate RL, McCoy JM, Pepinsky RB (2004) LINGO-1 is a component of the Nogo-66 receptor/p75 signaling complex. Nat Neurosci 7(3):221–228. https://doi.org/10.1038/nn1188

Niederost B, Oertle T, Fritsche J, McKinney RA, Bandtlow CE (2002) Nogo-A and myelin-associated glycoprotein mediate neurite growth inhibition by antagonistic regulation of RhoA and Rac1. J Neurosci 22(23):10368–10376

Osaki T, Shin Y, Sivathanu V, Campisi M, Kamm RD (2017) In vitro microfluidic models for neurodegenerative disorders. Adv Health Mater. https://doi.org/10.1002/adhm.201700489

Robaszkiewicz K, Ostrowska Z, Marchlewicz K, Moraczewska J (2016) Tropomyosin isoforms differentially modulate the regulation of actin filament polymerization and depolymerization by cofilins. FEBS J 283(4):723–737. https://doi.org/10.1111/febs.13626

Schevzov G, Bryce NS, Almonte-Baldonado R, Joya J, Lin JJ, Hardeman E, Weinberger R, Gunning P (2005) Specific features of

neuronal size and shape are regulated by tropomyosin isoforms. Mol Biol Cell 16(7):3425–3437

Schevzov G, Fath T, Vrhovski B, Vlahovich N, Rajan S, Hook J, Joya JE, Lemckert F, Puttur F, Lin JJ, Hardeman EC, Wieczorek DF, O'Neill GM, Gunning PW (2008) Divergent regulation of the sarcomere and the cytoskeleton. J Biol Chem 283(1):275–283

Schevzov G, Curthoys NM, Gunning PW, Fath T (2012) Functional diversity of actin cytoskeleton in neurons and its regulation by tropomyosin. Int Rev Cell Mol Biol 298:33–94. https://doi.org/10.1016/B978-0-12-394309-5.00002-X

Weinberger R, Schevzov G, Jeffrey P, Gordon K, Hill M, Gunning P (1996) The molecular composition of neuronal microfilaments is spatially and temporally regulated. J Neurosci 16(1):238–252

Yang IH, Siddique R, Hosmane S, Thakor N, Hoke A (2009) Compartmentalized microfluidic culture platform to study mechanism of paclitaxel-induced axonal degeneration. Exp Neurol 218(1):124–128. https://doi.org/10.1016/j.expneurol.2009.04.017